Structural, optical and morphological properties of zinc oxide (ZnO) nanosheets elaborated by hydrothermal method associated with microwave heating

N. BOUKHANOUFA[a], S. RAHMOUNI[b,c,*]
[a]*Electronic Department, University of Batna 2, Batna 05000, Algeria*
[b]*Higher School for Professors of Technological Education (ENSET) Skikda, 21300, Algeria*
[c]*Laboratory of Physical Chemistry and Biology of Materials (LPCBM) ENSET-Skikda, Algeria*

In this paper, the low temperature microwave assisted hydrothermal technique has been used to elaborate ZnO nanosheets by so-called soft chemistry and zinc acetate, as a source. In particular, we focused on the influence of elaboration parameters such as concentration, temperature, and time on the structural, morphological and optical properties ZnO nanosheets. X-ray analysis confirmed that the material has crystallized in hexagonal Wurtzite structure and the diffraction peaks in the case of higher precursor concentration are more intense and narrower, implying that the ZnO is better crystallized. The morphological characterization of the elaborated samples is performed using Scanning Electron Microscopy (SEM). It is revealed that the obtained powders are nano-platelets with irregular shapes and sizes and randomly arranged. The measured average thicknesses and diameter range are 38 nm and [50 nm - 600 nm], respectively. Moreover, the photoluminescence technique is used to investigate the optical behavior of the developed samples. Different photoluminescence bands are observed. The appearance of two peaks is recorded. The first corresponds to the upper limit of UV luminescence (394-400 nm) with a gap of (3.1 eV- 3.18 eV) around 394 nm. On the other hand, the second peak less intense and less broad is situated approximately in the middle of the visible blue band at 466 nm (blue: 466 – 500 nm) and a gap of (2.4 eV-2.6 eV) in the visible range (blue). The interesting properties of the developed structure enable it to be a potential alternative material for low-cost and high performance optoelectronic and photovoltaic applications.

(Received September 28, 2019; accepted October 21, 2020)

Keywords: Microwave heating, Hydrothermal route, ZnO powders, Nanosheets, Photoluminescence

1. Introduction

The development of nano objects from synthetic chemistry routes is nowadays one of the most important areas of fundamental and applied research. Zinc oxide (ZnO) is an n-type semiconductor component with a large direct gap Eg = 3.37 eV and therefore transparent and with a significant excitonic bonding energy of the order of 60 meV. Recently, the one-dimensional nanostructures (1D) of ZnO such as, nanotubes [1], nanowires [2], nanorods [3], nanobelts [4], nano-platelets [5] and nanosheets [6] are at the center of many studies and publications, due to their importance in fundamental physics studies and their potential applications in nanoelectronics, nanomechanics, and flat panel displays. Particularly, the optoelectronic device application of 1D ZnO nanostructure becomes one of the majorgoalin recent nanoscience researches [7].

Because of their physical, optical and electrical properties, high chemical and thermal stability, non-toxicity and abundance in nature, a great interest in studying ZnO nanostructures has been initiated. ZnO nanocrystal has found numerous applications, such as UV photodetectors [8], acoustic devices, [9] solar cells [10], photocatalysts [11], gas sensors [12], ultraviolet lasers [13], optoelectronic devices [14] and light emitting diode [15].

Several methods for the preparation of nanosized ZnO have been developed such as chemical vapor deposition [16], spray pyrolysis [17], sol-gel [18], hydrothermal methods [19]. It is noted here that hydrothermal synthesis is classified among the chemical methods and it has remarkable advantages in comparison with the usual techniques, for example: it is a simple technique, economic process (low cost), it allows to elaborate thin films or powders at low temperatures and large-scale industrial.

Microwave-hydrothermal reaction has been used as an effective method for the synthesis of nanoparticles of various oxides [20]. Compared with conventional methods. The microwave assisted hydrothermal method can save a lot of energy and time, and therefore reduce the price of the final product obtained

The adaptation of the hydrothermal synthesis to the microwave heating mode dates to the early 1990s. This technique brings an appreciable saving of time. It takes at least 24 hours to achieve a synthesis by conventional means, a few tens of minutes are enough to obtain a comparable result by microwave. Since 2000, work has also increased in the field of synthesis of materials and nanomaterials by microwave heating. In the present work, we investigate the effect of precursor concentration, reaction time and hydrothermal temperature on the

physical properties of ZnO nanosheets elaborated via microwave hydrothermal process.

2. Experimental details

2.1. Elaboration of ZnO nanosheets

Different quantities of zinc acetate ehydrate [($ZnCH_3COO_2$).$2H_2O$](0.3-.5 g) are dissolved in 35 ml of bidistilled water. The pH value of the solution is adjusted to 12 by adding 15 ml of 2M NaOH solution under stirring for 30 minutes using a magnetic bar in order to get a homogeneous solution and to ensure a better solubility of zinc acetate. The resulting solution is then transferred into 75 mL Teflon-lined autoclave and kept under 120 °C and 140 °C for various times in 900-Wdomestic microwave oven. The resulting white precipitates are collected and washed with distilled water and ethanol, then dried for 18 hours at 90 °C under atmospheric air.

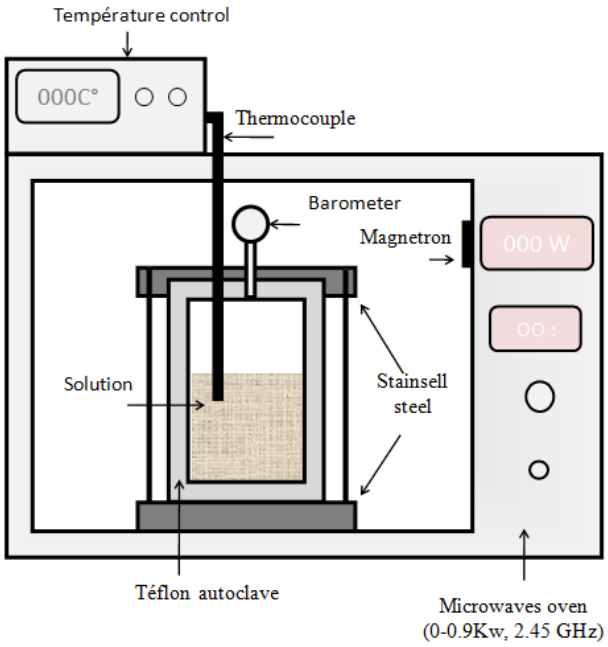

Fig. 1. Schematic sketch of ZnO nanopowders preparation by microwave hydrothermal synthesis

2.2. Characterizations techniques

Several characterization techniques have been used to identify the obtained materials. In this context, X-ray diffraction (XRD, Bruker AXS-8D diffractometer) with Cu Kα radiation (Cu Kα = 0.1541 nm) is used to study the structural properties. The morphology of our powders is examined using environmental scanning electron microscopy (ESEM, Philips XL 30 FEG). The optical properties of the prepared material are analyzed by photoluminescence (PL) at room temperature on a Perkin Elmer LS 55 spectrophotometer using a 325 nm xenon laser as the excitation light source.

3. Results and discussion

3.1. Structural properties

The X-ray diffraction spectrum of ZnO powders produced by the microwave-assisted hydrothermal technique and for different concentrations of zinc acetates, at fixed time and temperature values, is presented in Fig. 2.

In Fig. 2, concentrations of zinc acetate including (C_1= 1g and C_2= 1.5g) and for similar time (60 min), at both temperatures T1= 120 °C and T2=140 °C, lead to highly crystallized ZnO nanopowders and the diffraction peaks can be indexed unambiguously to the pure hexagonal Wurtzite phase–type ZnO consistent well with the standard PDF data base (JCPDS file 36-1451). The characteristic peaks are higher in intensity and narrower in spectral width, which indicate that the products possess good crystallinity.

No other peaks corresponding to impurities are detected, confirming that the final products are purely composed of ZnO. We would like to mention that the first sample with 0.3 g concentration and short time has not generated white precipitate, which is the elaborated compound subject of this study. While for the other two remaining samples (1.0 g and 1.5 g), we have obtained such powder and for this reason we have provided clarifications only for these two samples.

By using Scherrer's formula: ($D = k\lambda/B \cos\theta$, where D the average crystallite size of the powder, λ the wavelength of Cu-Kα (λ = 1.54178 Å), B the total width at mid-maximum intensity (FWHM) of the peak in radian, θ the diffraction angle of Bragg and k a constant [21], the crystallite size was determined. According to the diffraction peaks (101), (100) and (002) the average sizes of the crystallites are summarized in Table 1.

According to the XRD diffractogram (Fig. 3a), and in the case where the amount of precursor is 0,3 g, the prolonged reaction time is 1 hour and temperature is 120°C, respectively, itis found that several sharp diffraction peaks have occurred. This implies that the chemical reaction is not completed yet and intermediate compounds such as $Zn(OH)_2$ and $Zn(OAC)_2$were recorded, in addition to the appearance of peaks corresponding to ZnO. So, it can be concluded that under these presented experimental conditions lower concentration (0.3 g of zinc acetate) and shorter time, there is no white precipitate formation.

According to the spectrum of Fig. 3b, we observe that the intensity of ZnO peaks increases as function of the diffraction angle and are more intense in comparison with the spectrum of Fig. 3a. While, the intensity of the peaks of zinc acetate and zinc hydroxide (impurities) decreases. This phenomenon can be attributed to an incomplete chemical reaction, and ZnO cannot be developed for low concentrations. Furthermore, the crystallinity of the final product is significantly affected by the experimental factors such as concentration of the precursor and hydrothermal parameters (i.e. time and temperature).

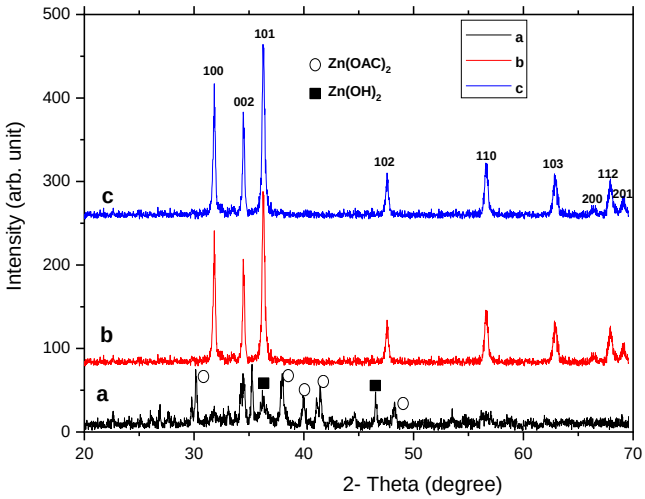

Fig. 2. X-ray diffraction of the ZnO nanopowders elaborated for various zinc acetate concentrations: (a) 0.3g, (b) 1g and (c) 1.5g and hydrothermal parameters 60min at 140°C (color online)

Table 1. Average crystallite sizes "D" values of ZnO particles

C_2=1.5g, T_2=140°C, t=60 min	
(hkl)	crystallite sizes "D"
(101)	29 nm
(100)	32 nm
(002)	37 nm

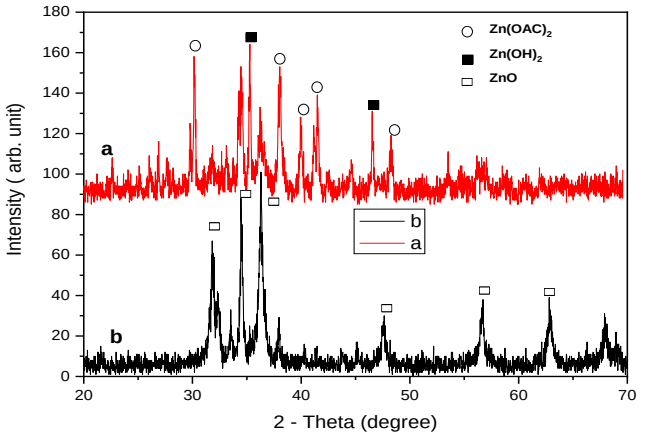

Fig. 3. X-ray diffraction of the ZnO nanopowders elaborated with dose of zinc acetate equal to 0.3 g for 60 min at two temperature values (a) 120°c and (b) 140°c (color online)

3.2. Morphological characterizations

Fig. 4 shows SEM images of the final ZnO products prepared at 140 °C reaction temperature and 1 hour as reaction time, using various amounts of zinc acetate dehydrates $Zn(OAc)_2.2H_2O$, 0.3 g, 1 g, 1.5 g, respectively denoted as (a), (b), (c). According to SEM observation, the sheets present an irregular shape and size. In Fig. 4c we show that for a maximum concentration of zinc acetate (1.5 g) nanosheets appeared in the products with 50 – 600 nm in diameter and about 38 nm in the thickness, confirming the results of the XRD analysis (Figs. 2, 3 and Table 1), which states that for low concentrations, the average thickness varies from 8 to 22 nm.

The crystallinity and size of the manufactured ZnO nanostructures are strongly influenced by the starting precursor concentration. The growth of ZnO from zinc acetate precursor dehydrate according to the hydrothermal technique is generally subjected to two stages, such as nucleation and growth in strongly alkaline solution (NaOH, pH = 12) and with the dissolution of $Zn(OAc)_2$, a sufficient amount of zinc hydroxide can be produced. The basic reaction mechanisms are given below:

$$NaOH \rightarrow Na^+ + OH^- \quad (1)$$

$$Zn(CH_3OO)_2 \rightarrow Zn^{2+} + 2(CH_3OO)^- \quad (2)$$

$$Zn^{2+} + 2OH^- \leftrightarrow Zn(OH)_2 \quad (3)$$

$$Zn(OH)_2 \leftrightarrow ZnO + H_2O \quad (4)$$

$$ZnO + H_2O + 2OH^- \leftrightarrow [Zn(OH)_4]2- \quad (5)$$

According to the reaction (Eq.4), ZnO nuclei are formed spontaneously when the concentration of Zn^{2+} or OH^- ions exceeds the saturation values. This is due to the fact that Zn^{2+} and OH^- are the most ionic species in solution, which have a very important role in the nucleation process. Several research studies have confirmed that the formation of ZnO nanosheets is favored when the pH value of the solution is too high. So, in our case, the Ph value of the solution was adjusted to 12 in order to satisfy such constraint of formation. Therefore, the formation of the above-mentioned nanosheets is probably due to the considerable inhibition of crystal growth of the c polar faces by sorption of OH^- ions. A reaction between OH- and Zn^{2+} ions on the c polar faces gives rapid growth in a long (002) direction. However, an electrostatic shielding effect can occur and inhibit the usual rapid growth along the *c* axis when the concentration of these exceeds a certain limit. It would contribute to the development of a long non-polar axis such as (100) and (101) [6,19].

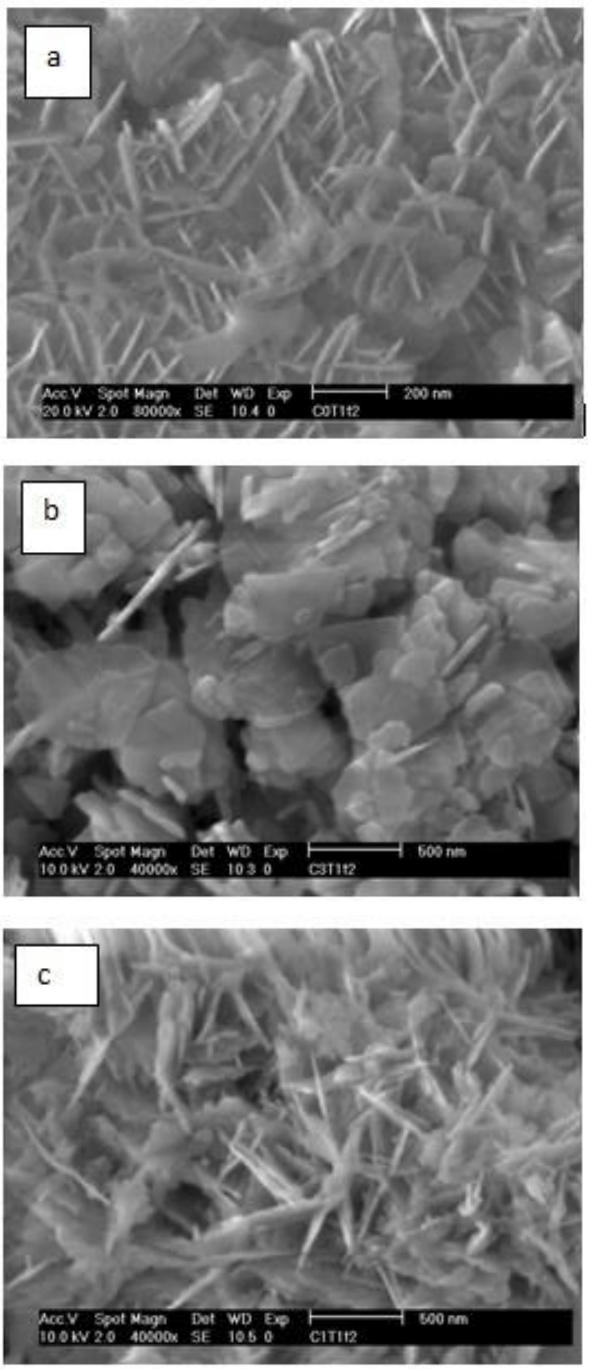

Fig. 4. SEM micrograph visualization of ZnO nanosheets fabricated at 140 °C for 60 min using various zinc acetate concentrations: (a) 0.3 g, (b) 1 g and (c) 1.5 g

3.3. Optical characterization

The PL spectra at room temperature of the ZnO powders developed, by the microwave assisted hydrothermal method, under several concentrations of zinc acetate and under fixed hydrothermal conditions (time and reaction temperature), are illustrated by Fig. 5. They are obtained using an excitation source with a wavelength of the order of 325 nm.

It is clearly observed that the PL spectra of all the samples have the same characteristics. The as-synthesized ZnO displays two emissions: an ultraviolet (UV) emission, called also, the near band edge emission (NBE) which is intense and broad centered in the range of (394-400 nm) (3.1eV - 3.18eV) generally originates from the direct recombination of the free excitons [22]. The second visible blue emission is located approximately at 466 nm (2.6 eV), which corresponds to a narrow, and stable visible blue emission band. The presence of this emission may be caused by the structural defects, such as oxygen vacancies and zinc interstitials in the crystalline ZnO [23]. From Fig. 5, it is clearly observed that the UV band is more intense than the defect band indicating good stochiometry.

In addition, regarding the appearance of blue luminescence in nanomaterials of ZnO. Dai et al. [24] have reported that blue emission at 466nm can exist due to the different intrinsic defects in ZnO films. More precisely, the atomic displacement of the constituents of the material such as the interstitial atoms of zinc acting as a level acceptor or oxygen vacancies may play the role of a donor level in stoichiometric ZnO powders [25].Visible luminescence is due to defects that are related to deep-level emissions, such as zinc interstitials and the oxygen deficiency. Study of the photoluminescence properties of ZnO nanomaterials in the visible region can provide information on the quality and purity of the material [26-29].

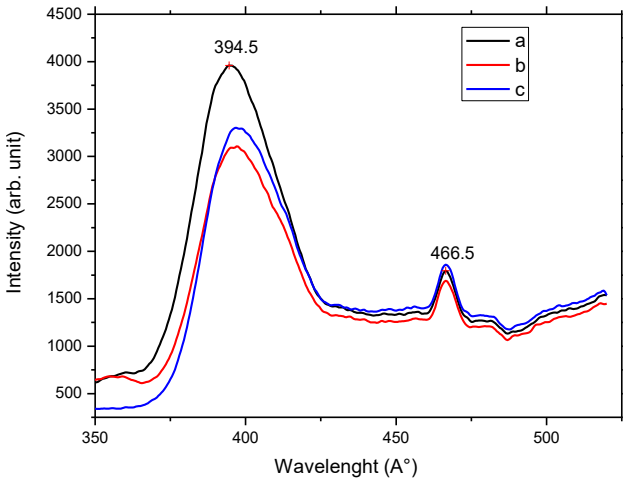

Fig. 5. Room temperature PL spectra of typical as-synthesized ZnO nanosheets elaborated at 140 °C for 60 min having several zinc acetate concentration: (a) 0.3 g, (b) 1 g and (c) 1.5 g (color online)

4. Conclusion

In this work, we have succeeded in elaborating nano-platelets of ZnO using hydrothermal process assisted by low temperature microwaves. The structural, morphological and optical properties of the elaborated samples were investigated using XRD, SEM and photoluminescence techniques. The X-ray analysis shows that the principal lines are those of the Wurtzite hexagonal ZnO, and their relative intensities indicate a crystalline growth in different planes. The photoluminescence spectra

show that the samples have the same emission profiles, the appearance of two peaks, the first one corresponds to the upper limit of the UV luminescence (394-400 nm) with a gap of (3.1eV - 3.18eV). The second peak is located approximately in the middle of the 466 nm blue visible band. This is due to the intrinsic defects. Therefore, these interesting properties of such developed structures enable them to be considered as a potential alternative material for low-cost and high performance optoelectronic and photovoltaic applications.

References

[1] J. Maria et al., Applied Catalysis A: General **551**(5), 71 (2018).
[2] Y. F. Zhu, I. Zhou, Q. S. Jiang, Ceramics International **46**(1), 1158 (2020).
[3] X. Liu, C. C. Mxene, Materials Letters **261**(15), 127127 (2020).
[4] Y. Xi, C. G. Hu, X. Y. Han, Solid State Communications **141**(9), 506 (2007).
[5] Q. Xu, Z. Zhang, R. Hong et al., Materials Letters **105**(15), 206 (2013).
[6] Qun Ma, Yongqian Wang, Junhan Kong, Hanxiang Jia, Jun Han, Optoelectron. Adv. Mat. **10**(9-10), 728 (2016).
[7] Sun Guipeng, Yan Jinliang, Niu Peijiang et al., Journal of Semiconductors **37**(2), 023005 (2016).
[8] H. Ferhati, F. Djeffal, Superlattices and Microstructures **134**, 106225 (2019).
[9] L. Rana, R. Gupta, A. Sharmal, M. Tomar, V. Gupta Journal Ferroelectrics **535**(1), 41 (2018).
[10] Ferhati, H., F. Djeffal, K. Kacha, Optik-International Journal for Light and Electron Optics **153**, 43 (2018).
[11] Y. Lin, Haiyang Hu, Applied Surface Science **502**(1), 144202 (2020).
[12] V. Singh Bhati, M. Hojamberdiev et al., Energy Reports **6**, Supplement (4), 46 (2020).
[13] F. Yang, J. Guo, L. Zhao et al., Nano Energy **67**, 104210 (2020).
[14] H. Ferhati et al., Materials Science in Semiconductor Processing **110**, 104957 (2020).
[15] B. O. Jung, Y. H. Kwon, D. Ju Seo et al., Journal of Crystal Growth **370**(1), 314 (2013).
[16] R. Bhujel, S. R. Bibhu, P. Swain, Materials Science in Semiconductor Processing **102**(1), 104592 (2019).
[17] K. Ravichandran, A. Jansi Santhosam, M. Sridharan, Surfaces and Interfaces **18**, 100412 (2020).
[18] P. Vlazan, C. I. Moisescu, I. Miron, P. Sfirloaga, I. Grozescu. Optoelectron. Adv. Mat. **9**(9-10), 1139 (2015).
[19] S. Agarwala, P. Rai, E. N. Gatell, Sensors and Actuators B: Chemical **292**(1), 24 (2019).
[20] A. Mirzaei, G. Neri, Sensors and Actuators B; Chemical **237**, 749 (2016).
[21] H.-C. Kao, W. C. Wei, J. Am. Ceram. Soc. **83**(2), 362 (2000).
[22] E. Nurfani, R. Kurniawan, T. Aono et al., Japanese Journal of Applied Physics **56**(11), 112101 (2017).
[23] J. Wang, R. Chen, L. Xiang, Ceramics International **44**(7), 7357 (2018).
[24] J. Dai, Mao-Hui Yuan, Jian-Hua Zeng et al., Optics Express **23** (22), 29231 (2015).
[25] V. Sharma, T. Kumar Das, P. Ilaiyaraja et al., Solar Energy **191**, 400 (2019).
[26] D. Li, Y. H. Leung, A. B. Djurišića et al., Appl. Phys. Lett. **85**(9), 1601 (2004).
[27] N. L. Tarwal, V. V. Shinde, A. S. Kamble et al., Applied Surface Science **257**(24), 10789 (2011).
[28] S. Muthukumaran, R. Gopalakrishnan, Optical Materials **34**(11), 1946 (2012).
[29] S. A. Azzez, Z. Hassan, J. J. Hassan et al., Journal of Luminescence **192**, 634 (2017).

*Corresponding author: rahmouni.eln@gmail.com